Three Faceted COLLECTOR SPECIMENS

Three stones recently submitted to GIA (figure 1) were found to be rare mineral species that had not previously been examined at the Carlsbad laboratory. Standard gemological testing and Raman analysis identified these specimens as wagnerite, thaumasite, and strontianite.

A 0.60 ct transparent golden yellow pear brilliant cut with vitreous luster was identified as the phosphate monoclinic crystal wagnerite, $(Mg,Fe^{2+})_2(PO_4)F$. Though uncommon, wagnerite occurs in various geologic settings, such as granitic pegmatites, gneisses, eclogites, and hydrothermal environments (P. Korbel and M. Novak, *The Complete Mineral Encyclopedia*, Gramercy, Lisse, the Netherlands, 2003). It had a specific gravity (SG) of 3.15, a refractive index (RI) of 1.568–1.580, and a biaxial positive optic nature. Wagnerite is a relatively soft and brittle mineral with a Mohs hardness of 5.0–5.5. The stone was inert under both long-wave and short-wave UV radiation. Multiphase fluid inclusions, fingerprints, graining, and color zoning features were observed with magnification.

The largest stone, a 1.72 ct transparent colorless octagonal step cut, had a relatively low SG of 1.90, an RI of 1.470–1.515, and a biaxial negative optic nature. It was inert to long-wave and short-wave UV. These properties, along with Raman testing, led to its identification as thaumasite, a silicate mineral with the chemical formula $Ca_3(SO_4)[Si(OH)_6](CO_3)\cdot 12H_2O$ belonging to the hexagonal crystal system. Magnification revealed strong doubling, spectacular radiating fibrous inclusions, reflective films, tiny crystal inclusions, and strong hexagonal angular graining. Thaumasite has a vitreous luster and a brittle nature due to its low hardness of 3.5 on the Mohs scale. Thaumasite occurs in geothermal waters or seawaters reacting with basalt and tuffs, or in areas of contact metamorphism (J.W. Anthony et al., *Handbook of Mineralogy: Volume II: Silica, Silicates: Part 2*, Mineral Data Publishing, Tucson, Arizona, 1995, p. 790).

Figure 1. Left to right: 0.60 ct golden yellow wagnerite, 1.72 ct colorless thaumasite, and 1.41 ct pale yellow strontianite.

The last stone we observed was a transparent pale yellow octagonal step cut with vitreous luster. It proved to be strontianite, $SrCO_3$, an orthorhombic carbonate mineral member of the aragonite group with a Mohs hardness of 3.5. The 1.41 ct specimen was highly birefringent, with an RI of 1.511–1.661, an SG of 3.76, and a biaxial negative optic nature. It fluoresced red under long-wave UV but displayed a weak whitish reaction under short-wave UV. The stone exhibited strong doubling and fluid inclusions under magnification. Raman spectroscopy confirmed its identity. Strontianite occurs together with calcite and zeolites in hydrothermal, low-temperature veins and in cavities of volcanic rocks (Korbel and Novak, 2003).

Wagnerite, thaumasite, and strontianite are rarely seen as faceted gems due to their softness and brittleness. These collector specimens were the first of their kind to be submitted to

Editors' note: All items were written by staff members of GIA laboratories.

Gems & Gemology, Vol. 53, No. 1, pp. 90–101.

GIA's Carlsbad laboratory for testing. Although challenging to identify without advanced testing techniques, they bring excitement to gemologists searching for unusual faceted gems.

Jonathan Muyal and Nicole Ahline

Unusual Dark Orangy Red CORDIERITE

The New York lab recently examined the transparent dark orangy red cordierite shown in figure 2. Cordierite, a magnesium aluminum cyclosilicate with the formula $Mg_2Al_4Si_5O_{18}$, is better known by its gemological name of iolite, which comes from the Greek *ios* (violet). The term is reserved for the violet through slightly violetish blue gem-quality variety of cordierite. Iolite's typical colors have been compared to blue sapphires and tanzanites. These colors are thought to come from the charge transfer between Fe^{2+} and Fe^{3+} ions.

The stone's RI ranged from 1.515 to 1.547, with a birefringence of 0.037. This refractive index is much lower than what is listed in the literature for iolite, and we believe the discrepancy is due to the stone's lower Fe content. SG was measured as 2.56. The stone showed strong trichroism ranging from orangy red to dark brown to purple. There was no fluorescence observed with exposure to long- and short-wave UV. Raman spectroscopy using 514 nm laser excitation conclusively identified the stone as cordierite (figure 3) with a strong match to the cordierite spectra in the RRUFF database (http://rruff.info).

Figure 2. This 8.13 ct cordierite had an unusual dark orangy red color.

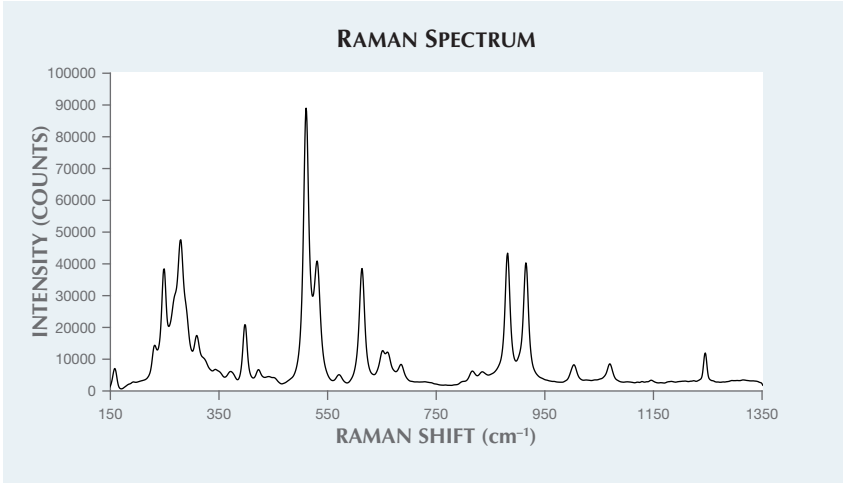

Figure 3. Raman spectroscopy identified the orangy red stone as a cordierite.

Microscopic examination with fiber-optic illumination revealed fingerprints, rows of flaky whitish inclusions, and large fractures throughout the stone that had been filled with an unknown clarity-enhancing material (figure 4). The larger surface-reaching fractures in the stone appeared to have a "heat wave" appearance (figure 4B), that could be characteristic of the clarity-enhancing material. Cordierite, which is structurally similar to beryl, will easily develop fractures and is commonly clarity enhanced with oil-based fluids. Both cordierite and beryl are structurally similar in that they are cyclosilicates,

Figure 4. Various inclusions within the dark orangy red cordierite. Numerous partially enhanced fractures are visible (B), along with low visibility on the surface (D). Field of view 4.77 mm (A), 14.48 mm (B), 3.57 mm (C), and 3.57 mm (D).

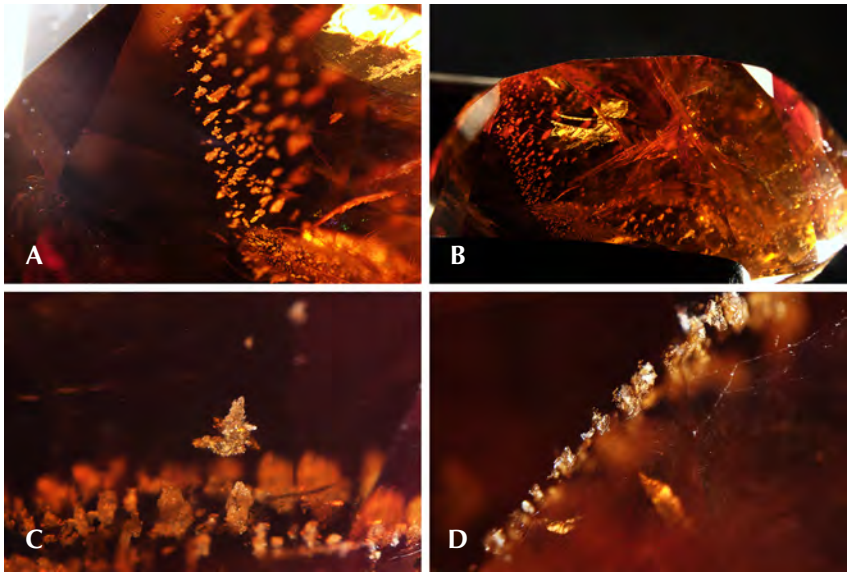

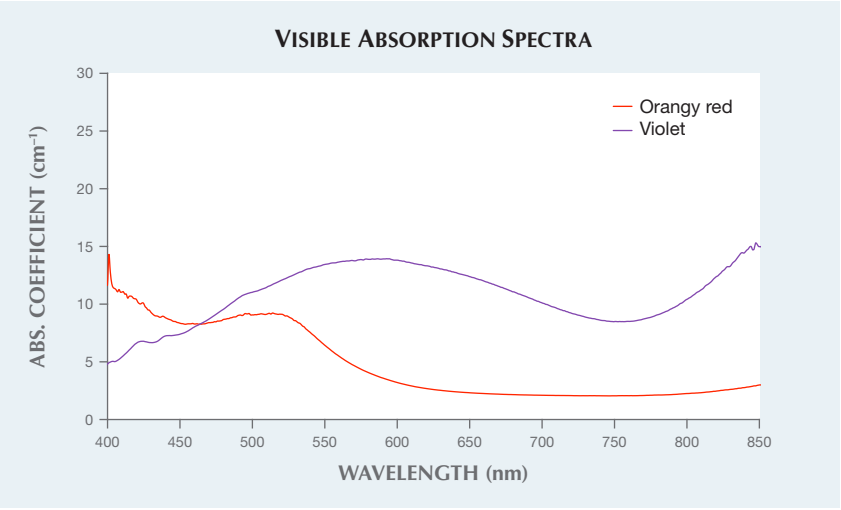

Figure 5. In these visible absorption spectra, notice the large window between 600 and 800 nm for the orangy red cordierite sample and the absorption band centered at 580 nm for the GIA reference spectrum of violet iolite.

containing linked six-member rings of tetrahedra that result in channels within the crystal structure. These channels are capable of trapping water along with cations such as from the alkali and alkaline earth metals. The high water content within the stone was represented by the strong overtone bands seen in the Fourier-transform infrared (FTIR) spectrum, with very similar features to that of hydrothermal natural beryl spectra. Laser ablation–inductively coupled plasma–mass spectrometry (LA-ICP-MS) detected trace levels of alkali and alkaline metals.

A similar red cordierite, examined in December 2015, was said to be from the Iakora district of Fianarantsoa Province in southeast Madagascar (Spring 2016 GNI, pp. 97–98). The visible absorption spectrum we observed was similar to the one described by Fritsch et al. (figure 5). The spectrum had a decrease in absorption in the 400–500 nm region and low absorption between 600 and 800 nm, resulting in a transmittance window in the orange to red region that produced the color of the stone. These regions of low absorption are characteristic of the trichroic color components noted in the stone. We compared this visible spectrum to a GIA reference spectrum of ordinary iolite. The violet color of iolite is produced by a strong absorption band centered at approximately 580 nm, resulting from intervalence charge transfer to either valence state of Fe cations that might have occupied the divalent and trivalent sites in the crystal structure (substituting for Mg and Al, respectively; see M. O'Donoghue, *Gemstones*, Chapman and Hall Ltd., London, 1988, p. 77). Although the red cordierite contained a considerable amount of iron, this charge transfer did not appear to be taking place. The potential causes of the color are still unknown but can be linked to manganese (up to 486 ppmw in the orangy red sample and 248 ppmw in the violet sample) or iron, both of which were detected by LA-ICP-MS. This orangy red cordierite appeared to have roughly half as much iron as a saturated violet iolite (approximately 25,000 and 40,000 ppmw, respectively). No other transition metals varied significantly between the orangy red and violet samples. Regardless of the origin of color for the orangy red cordierite, naming this variety "iolite" could be misleading according to the definition of the term.

This is the first time GIA has encountered a cordierite of this color.

Augusto Castillo and Akhil Sehgal

Cape DIAMOND with Yellow Phosphorescence

Phosphorescence in a cape diamond is very rare, especially after exposure to long-wave UV light. The New York laboratory recently examined a cape diamond exhibiting yellow phosphorescence after exposure to a long-wave UV source. The 0.75 ct Faint yellow-green round brilliant is shown in figure 6.

Cape absorption peaks were observed at 415 and 477 nm, along with a GR1 peak (figure 7, left). The IR spectrum confirmed that this was a type Ia diamond, with nitrogen aggregates detected in the one-phonon region. Hydrogen-related peaks were also detected at 1405, 2785, 3107, 3237, 4169, and 4496 cm^{-1}. Brown radiation stains were found on the girdle. The diamond contained contacted partially graphitized omphacite crystals with cuboctahedral morphology (figure 7, right). Strong blue fluorescence and medium yellow phosphorescence were observed under a desktop long-wave UV light source. Under short-wave UV, medium yellow fluorescence was noted but phosphorescence was absent. DiamondView imaging (<225 nm excitation) also showed greenish blue fluorescence but no phosphorescence. Fiber-optic illumination revealed the blue "transmission" luminescence that occurs when a

Figure 6. This yellow-green 0.75 ct cape diamond displayed yellow phosphorescence to long-wave UV light.

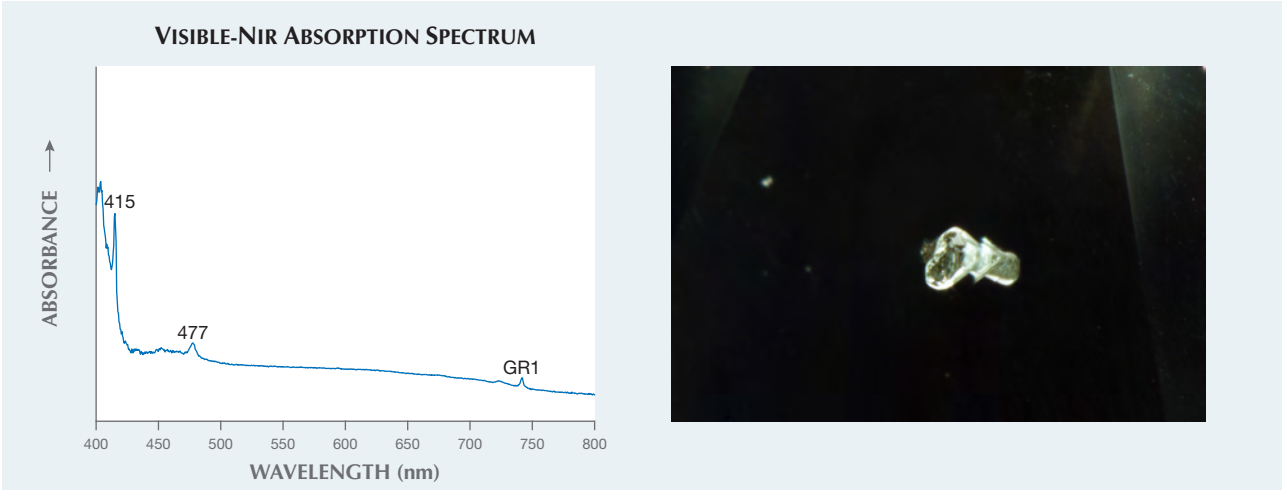

Figure 7. The diamond displayed "cape" absorption peaks at 415 and 477 nm along with a GR1 peak (left). It contained contact crystal inclusions of green omphacite (right; field of view 1.41 mm).

strong light travels through a diamond. The UV-Vis spectrum of such diamonds shows an absorption peak at 415 nm and a luminescence peak at the lower energy end of the peak. Such is the case with this stone.

Nearly 30 years ago, a bicolor diamond with a near-colorless central portion and light yellow tips was reported in *G&G* (Winter 1989 Lab Notes, p. 237). It showed very weak chalky yellow phosphorescence for approximately 10 seconds after the long-wave UV lamp was turned off. This yellow phosphorescence was observed throughout the stone regardless of its bicolor nature. Its central colorless region exhibited weak cape lines and strong blue transmission, similar to the green diamond in this note. Unlike our sample, the bicolor diamond also showed very weak yellow phosphorescence to short-wave UV. A chameleon diamond may display strong yellow phosphorescence to a long-wave UV light source (Summer 1992 Lab Notes, p. 124; Spring 2000 Lab Notes, pp. 60–61). Our sample was not a chameleon diamond, however.

Greenish yellow phosphorescence in a chameleon diamond has been systematically measured using a spectrometer (see S. Eaton-Magaña et al., "Fluorescence spectra of colored diamonds using a rapid, mobile spectrometer," Winter 2007 *G&G*, pp. 332–351). The peak maximum recorded for the chameleon diamond was 557 nm. We used an Ocean Optics USB2000 charge-coupled device (CCD) spectrometer similar to the one described in Eaton-Magaña et al. (2007), but with a different UV source. In place of a deuterium source, we used

Figure 8. Phosphorescence spectra (left) show a peak maximum at 570 nm, which is responsible for the cape diamond's yellow phosphorescence. Shown on the right is the phosphorescence decay curve at 570 nm.

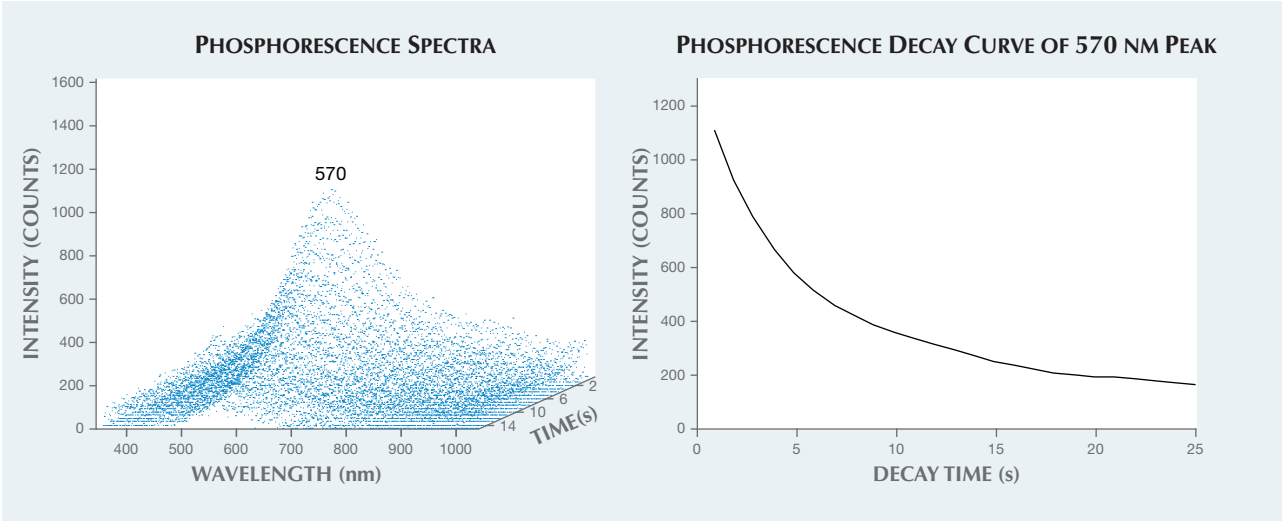

GIA's new LED desktop long-wave UV (365 nm excitation) light source. A broad peak at approximately 570 nm, which is responsible for the yellow phosphorescence, was observed in the emission spectra (figure 8, left). The phosphorescence decay curve at 570 nm, representing the rate of decreasing intensity with time, is plotted in figure 8 (right). Half-life is defined as the time required for the initial peak intensity to decrease to one-half its original value (again, see Eaton-Magaña et al., 2007). The half-life value measured for our sample was 5.0 seconds.

Yellow phosphorescence is a very rare feature in cape diamonds. The defect responsible for this optical feature remains unknown.

Kyaw Soe Moe, Jon Neal, and Paul Johnson

Pink SAPPHIRE Filled with Bismuth-Based Glass

Recently, GIA's Bangkok laboratory received a 2.77 ct light pink sapphire (figure 9) for an identification report. The sample was a semi-transparent cabochon with natural inclusion features: silk needles and particles, twinned planes, and thin films. Also observed throughout the stone were numerous gas bubbles of various shapes and sizes that were trapped along surface-reaching fractures and cavities (figure 10). These indicate the presence of glass filling. However, no flash effect was evident in the filled fractures. The stone's RI of 1.76 and UV fluorescence reaction (medium red to long-wave and weak red to short-wave) were consistent with corundum. Its SG of 3.87 was lower than that of corundum and possibly a result of the filler. Due to the sapphire's very light color, its visible-range absorption spectrum was difficult to observe.

Figure 9. This 2.77 ct light pink sapphire cabochon was treated with a bismuth-based glass filling.

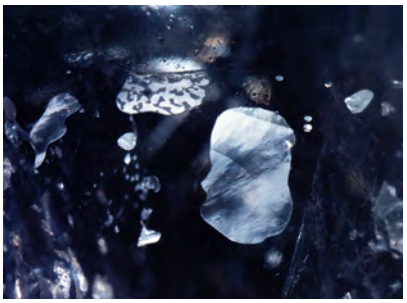

Figure 10. With the aid of fiber-optic illumination, magnification revealed these trapped gas bubbles of various shapes and sizes in the light pink sapphire. Field of view 2.00 mm.

Qualitative chemical analysis using energy-dispersive X-ray fluorescence (EDXRF) spectroscopy showed the presence of bismuth in addition to the expected Al, Cr, Fe, and Ga. No lead was detected in the sample, even with the aid of the thick palladium filter. The chemical composition of the filler indicated that the stone had undergone fracture filling using bismuth-based glass ("Ruby treatments – revisited, with Mozambique's perspective," *Lab Information Circular*, Gem Testing Laboratory, Vol. 63, December 2011). Due to the large difference in refractive indices between the bismuth-based glass filled area and the surrounding corundum, this treatment was easier to visually detect than lead-glass filling (figure 11).

Figure 11. Under reflected illumination, the pink sapphire's large cavity filling was readily visible with the unaided eye. Field of view 2.70 mm.

Fracture filling with lead glass and non-lead glass has been widely used in low-grade ruby (S.F. McClure et al., "Identification and durability of lead glass–filled rubies," Spring 2006 *G&G*, pp. 22–34). Pink sapphires such as this 2.77 ct stone are less commonly encountered in the laboratory for examination and identification.

Ratima Suthiyuth

First Observation of H4 Defect in CVD SYNTHETIC DIAMOND

Diamond consists of a relatively simple lattice of carbon atoms wherein only a few impurities can substitute into the structure. Despite the apparent simplicity, the diversity of defects that can exist in the diamond lattice is astounding. Nitrogen is the most abundant impurity in diamond; one of the defects commonly seen in natural diamonds, the H4 defect, consists of four nitrogen atoms and two vacancies. It is strongly associated with B-aggregated nitrogen impurities, which consist of four nitrogen atoms surrounding a single vacancy. H4 is created through a fairly straightforward formation mechanism where a single vacancy is trapped adjacent to a B-aggregate of nitrogen. H4 is often seen in irradiated and annealed diamonds with suitable amounts of B-form nitrogen, and is a mature aggregate of nitrogen that is very difficult to achieve in synthetic diamond growth or even post-growth treatment.

We were very surprised to observe an H4 peak at 496 nm in a pink synthetic diamond grown by chemical vapor deposition (CVD) that was recently submitted to GIA's Carlsbad laboratory for a synthetic colored diamond grading report. This 0.26 ct

Figure 12. This 0.26 ct pink synthetic diamond contains the first H4 defect GIA has observed in a CVD synthetic diamond.

round brilliant (figure 12) was type Ib (single substitutional nitrogen impurities) with a very low total nitrogen content and no detectable A or B form nitrogen. FTIR spectroscopy also showed a peak at 3107 cm^{-1}, indicating the presence of a defect consisting of three nitrogen atoms surrounding a vacancy along with a hydrogen atom.

In addition to the observation of the H4 defect (figure 13, left), the synthetic nature of the sample was revealed by the 737 nm SiV^- defect in the photoluminescence (PL) spectrum (figure 13, right). The presence of (subtle) growth layers in the DiamondView fluorescence images provided further confirmation. This diamond was grown using gas that was doped with nitrogen, allowing its incorporation into the diamond lattice as single substitutional nitrogen. The pink color was produced by NV^- centers created during post-growth irradiation and annealing treatment. Nitrogen aggregation from single substitutional nitrogen to the more complex B-form nitrogen requires very high temperatures and pressures: 2500°C and 9.5 GPa for several hours (I. Dobrinets et al., *HPHT-Treated Diamonds: Diamonds Forever*, Springer Science & Business Media, 2013, p. 41) and generally requires a high starting concentration of nitrogen. This CVD synthetic diamond had low total nitrogen content and was grown under vacuum and likely irradiated and annealed at atmospheric pressure, making the occurrence of H4 even more puzzling. It is possible that the H4 was created during the irradiation and annealing process, but among the many samples GIA has examined, this was the first observation of this defect in a CVD synthetic diamond.

Troy Ardon and Christopher M. Breeding

HPHT Synthetic Diamond Melee Without Si or Ni Defects

Near-colorless synthetic diamond melee grown using the high-pressure, high-temperature (HPHT) method have created significant concern in the industry, and various screening methods have been developed to take into account their most reliable distinguishing features. In general, the specimens described in previous Lab Notes (e.g. Summer 2015, pp. 183–184) were very small round faceted goods ranging between 0.005 and 0.01 ct.

Figure 14. These four near-colorless round brilliant melee were identified as HPHT synthetic diamonds lacking the typical Si- and Ni-related defects.

Recently GIA's Bangkok laboratory received four loose near-colorless round brilliants for quality assurance service (figure 14). They weighed between 0.07 and 0.09 ct, slightly more than previously submitted melee. All were identified as type IIb HPHT-grown material using FTIR spectrometry. Their most interesting feature was the absence of silicon- or nickel-related emission peaks when analyzed

Figure 13. Photoluminescence spectra of the pink CVD synthetic diamond showed the occurrence of an H4 defect (left) as well as a SiV^- defect (right).

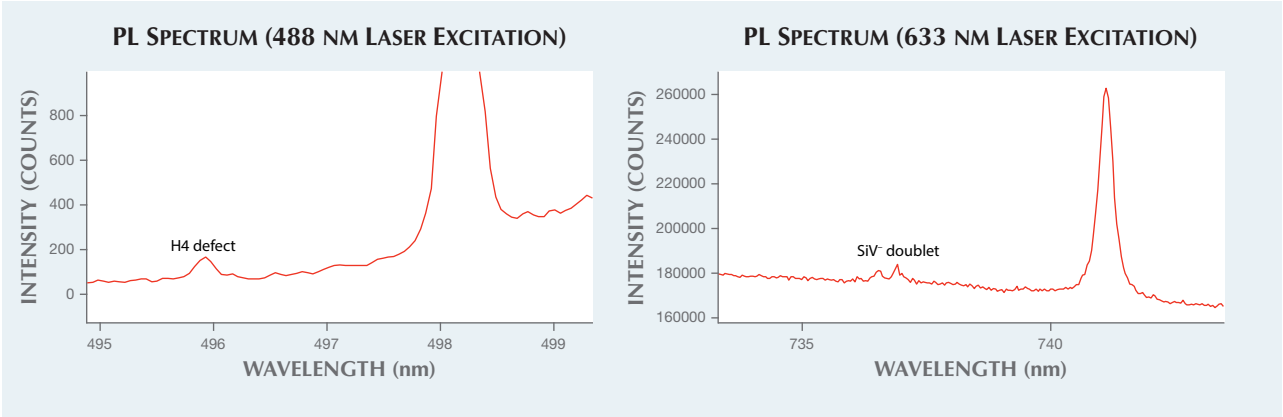

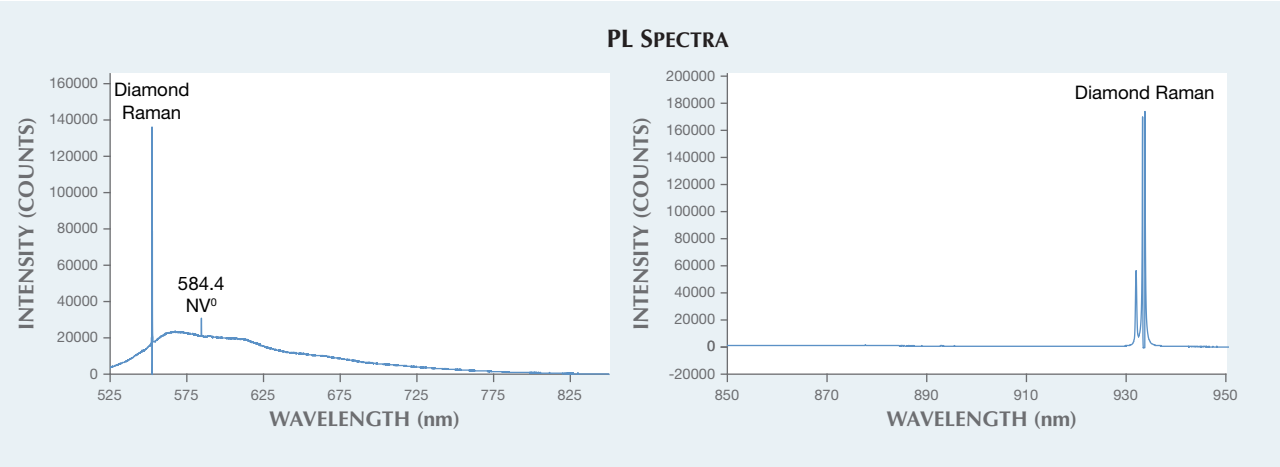

Figure 15. The PL spectra features observed at liquid nitrogen temperature lacked the 736.6/736.9 nm emission doublet related to the SiV^- defect (left, 514 laser excitation) and the Ni-related defect doublet at 883/884 nm (right, 830 nm laser excitation).

at liquid nitrogen temperature by PL spectroscopy (figure 15). The spectra typically observed in HPHT synthetic diamonds show an emission doublet related to the negatively charged silicon split-vacancy defect SiV^- at 736.6/736.9 nm and an associated Ni-related defect at 883.0/884.7 nm (Summer 2015 Lab Notes, pp. 183–185).

The growth patterns observed in the DiamondView were an identifying feature that did remain the same. The characteristic angular growth patterns and blue-green fluorescence, together with an associated green phosphorescence, still provide important evidence that aid in the separation of natural and synthetic diamonds (figure 16). Examination with a gemological microscope revealed metallic and rod-like inclusions (figure 17) that also assisted in identifying these melee as synthetic diamonds.

The study of these four melee-size HPHT synthetic diamonds revealed atypical PL spectra. However, other means of identification (inclusions, growth patterns as seen via the DiamondView, and their phosphorescence reactions) still played an important role in their identification. It is interesting to note that HPHT synthetic melee diamonds being submitted to GIA for identification are getting larger, indicating the continuous improvement of synthetic technology.

Piradee Sirithеerakul and Wuyi Wang

Figure 16. These DiamondView fluorescence and phosphorescence images of a 0.081 ct sample show growth patterns characteristic of HPHT synthetic diamond.

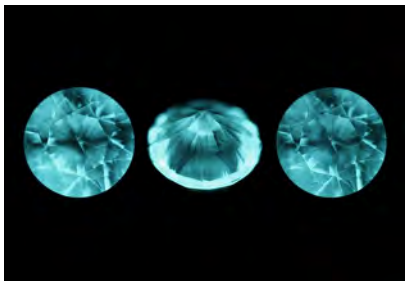

Figure 17. Darkfield illumination reveals rod-like inclusions in a 0.087 ct HPHT-grown melee diamond.

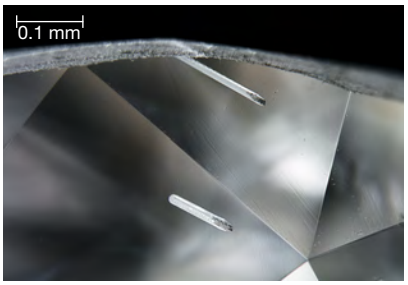

HPHT Synthetic Diamond with Intense Green Color

HPHT-grown synthetic diamonds are predominantly colorless, yellow, and blue, depending on the control of impurities during growth. Other colors are very rare. In this study, we report on an intensely colored green HPHT synthetic diamond identified in the New York laboratory.

This square-cut synthetic diamond, which weighed 0.42 ct and measured 4.42 × 4.34 mm with a depth of 2.59 mm, was graded as Fancy Deep green (figure 18). Initial observation revealed strong color zoning with narrow, colorless growth sectors on the pavilion that were visible without magnification. An abundance of small metallic inclusions observed under magnification (figure 19) caused the sample to exhibit magnetism. Magnetism is a common but not diagnostic feature in HPHT synthetic diamonds. Natural diamonds may also exhibit magnetism, though only in extremely rare cases (G.R. Rossman and J.L. Kirschvink, "Magnetic properties of gem-quality synthetic diamonds," Fall 1984 *G&G*, pp. 163–166).

Upon further examination, the diamond was determined to be type IIb (containing the impurity boron), as seen from its mid-FTIR absorption spectrum (figure 20). The concentration of uncompensated boron in this diamond was 0.013 ± 0.003 ppma.

Figure 18. This 0.42 ct green HPHT synthetic diamond displayed strong growth sectors that were observed without magnification.

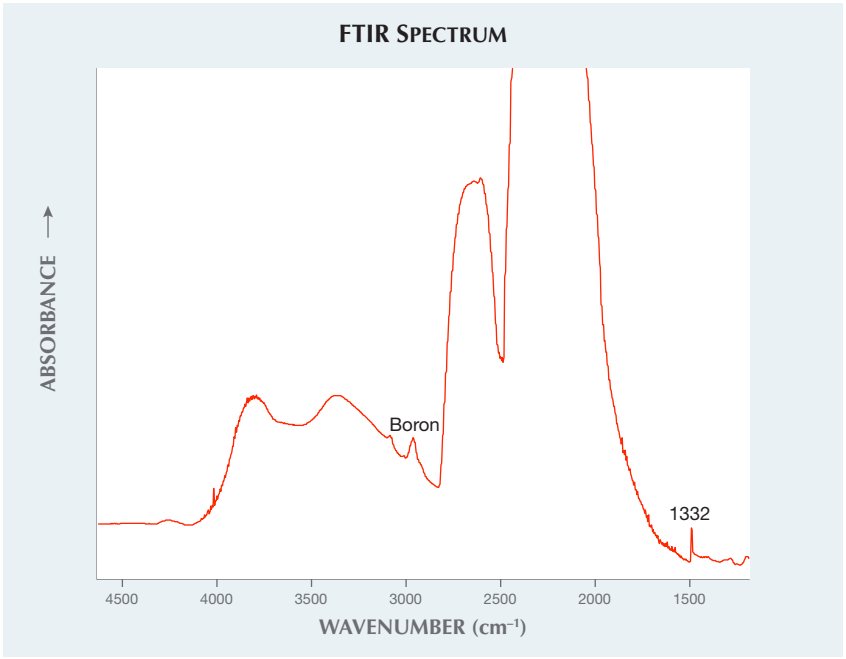

Figure 20. The green synthetic diamond's mid-FTIR spectrum, which determined that the material was type IIb, showed an uncompensated boron concentration at ~0.013 ppma.

This amount, though detectable, did not contribute to the green color. Many synthetic diamonds grown by New Diamond Technology (NDT) in Russia reportedly also contain this level of boron impurity, as it is incorporated during the growth process (B. Deljanin et al., "NDT breaking the 10 carat barrier," *Contributions to Gemology*, No. 15, 2015). DiamondView imaging revealed the typical hourglass growth structure of HPHT synthetic diamonds (figure 21), along with extremely strong phosphorescence for which the presence of boron might be responsible. Noted in the FTIR spectrum was an absorption feature related to nitrogen impurity, a relatively strong peak at 1332 cm^{-1} caused by N^+. It is unusual to see such features in today's synthetic diamonds. A UV-Vis-NIR absorption spectrum showed strong nickel-related absorption, with a band observed at ~685 nm (figure 22). This center, due to a Ni^+ interstitial vacancy, creates a "transparent" window at approximately 555–585 nm, resulting in an observed green color. This diamond was most likely HPHT treated post-growth to activate the Ni^+ and cause this intense absorption. It is very rare to see HPHT synthetic diamond with an intense green color attributed to a nickel-related impurity.

In addition to boron and nickel, this synthetic diamond also contained the SiV^- impurity in its crystal lattice. Recent studies have shown that while this impurity is common in CVD-grown diamonds, it may also be observed in HPHT-grown diamonds (U.F.S. D'Haenens-Johansson et al., "Near-colorless HPHT synthetic diamonds from AOTC Group," Spring 2014 *G&G*, pp. 30–45). The distribution of Si and Ni impurities were mapped using Raman mapping techniques, and the results proved consistent with previous studies of near-colorless HPHT-grown diamonds also observed in the trade (P. Johnson et al., "Discovery and distribution of the [Si-

Figure 19. The green synthetic diamond displayed strong magnetism, caused by abundant metallic inclusions. Field of view ~1.4 mm.

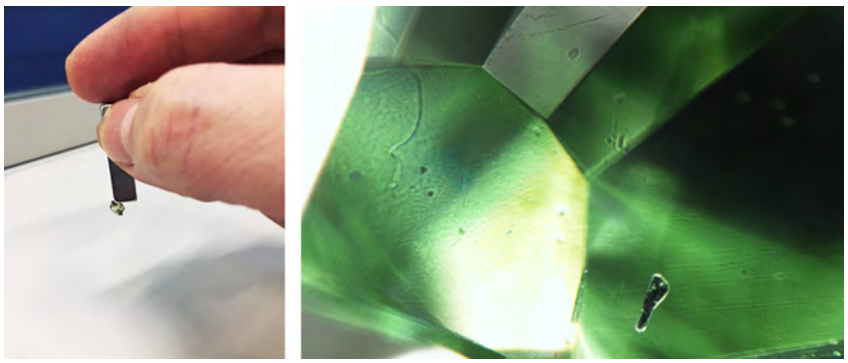

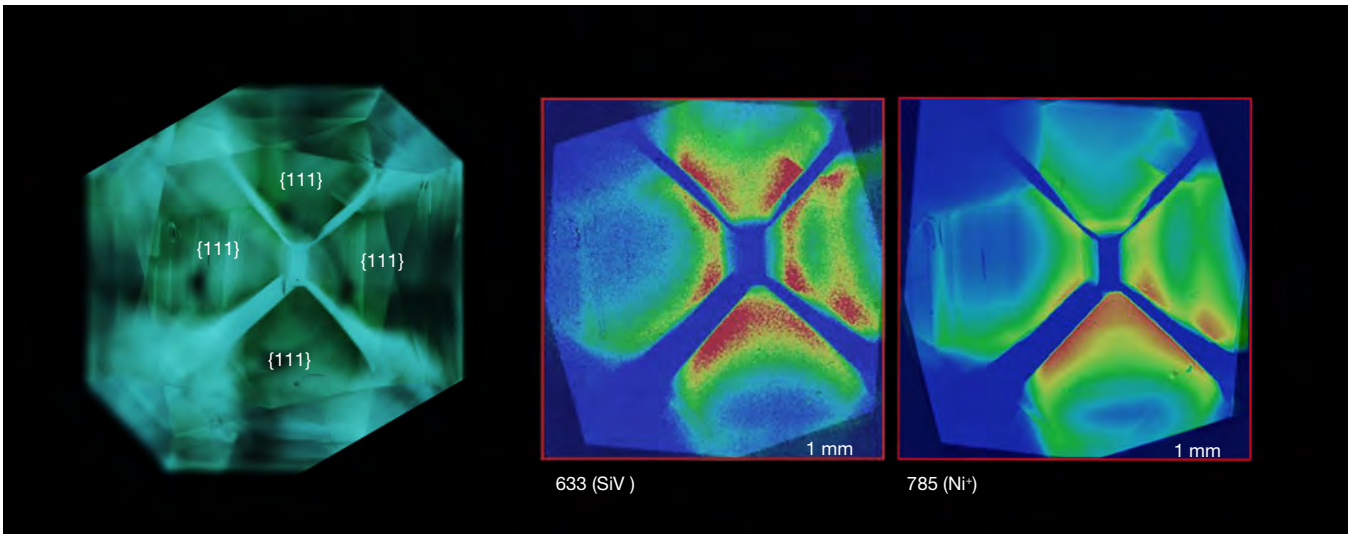

Figure 21. An oriented DiamondView image (left) and 633 and 785 nm PL maps (right) show the SiV^- and Ni^+ defects confined to the {111} growth sectors.

V]- defect in HPHT-grown gem-quality diamonds," 2015 GSA Annual Meeting, paper No. 300-12), with both the Ni^+ and SiV^- confined to the {111} growth sectors. Typically observed in HPHT-grown diamonds, these {111} sectors are the most developed and dominate the diamond crystal's morphology. The SiV^- center does not contribute to the color of these synthetic diamonds, and it is either intentionally or unintentionally incorporated during crystal growth (again, see figure 21).

These spectroscopic and gemological features, with the exception of the green color resulting from nickel, were consistent with typical HPHT synthetic diamond. This is the first instance in which nickel has been reported to contribute to the deep green color of a synthetic diamond. This finding could indicate a new development in growth technology and a new material making its way into the diamond trade. This example was submitted as an undisclosed synthetic diamond and was subsequently issued an identification report.

Developments in synthetic diamond growth technologies (both CVD and HPHT) continue to emphasize the need for careful observation and testing techniques to identify the new types of materials encountered in the gem trade today.

Paul Johnson and Elina Myagkaya

Figure 22. The HPHT synthetic diamond's UV-Vis-NIR spectrum displayed a very intense Ni-related absorption.

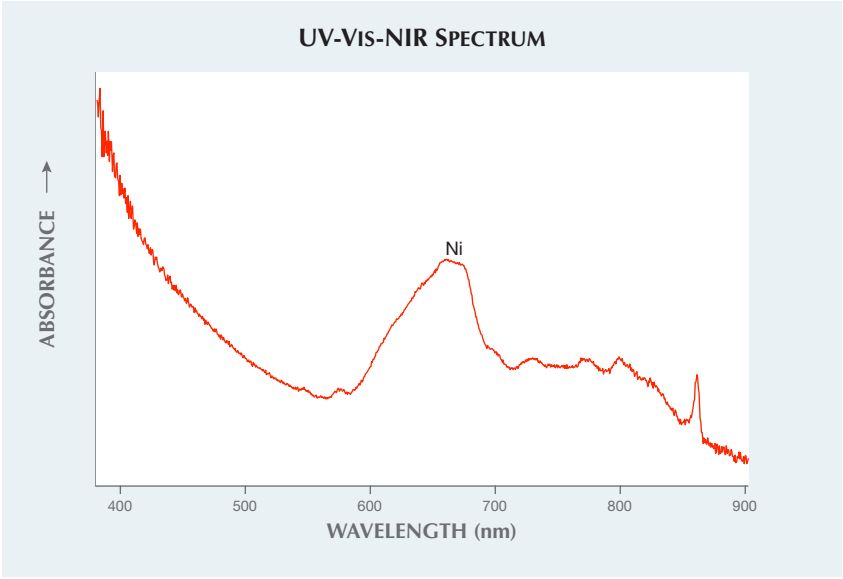

Multi-Elemental Diffused and Melt-Grown SYNTHETIC SAPPHIRE

GIA's Carlsbad laboratory examined a 4.21 ct faceted blue oval. Standard gemological testing determined that the stone was uniaxial negative and had an RI of n_ε = 1.759 and n_ω = 1.769, with a corresponding birefringence of 0.010. Hydrostatic SG was measured as 4.00. The stone was inert to long-wave UV and showed medium chalky blue color to short-wave UV. These

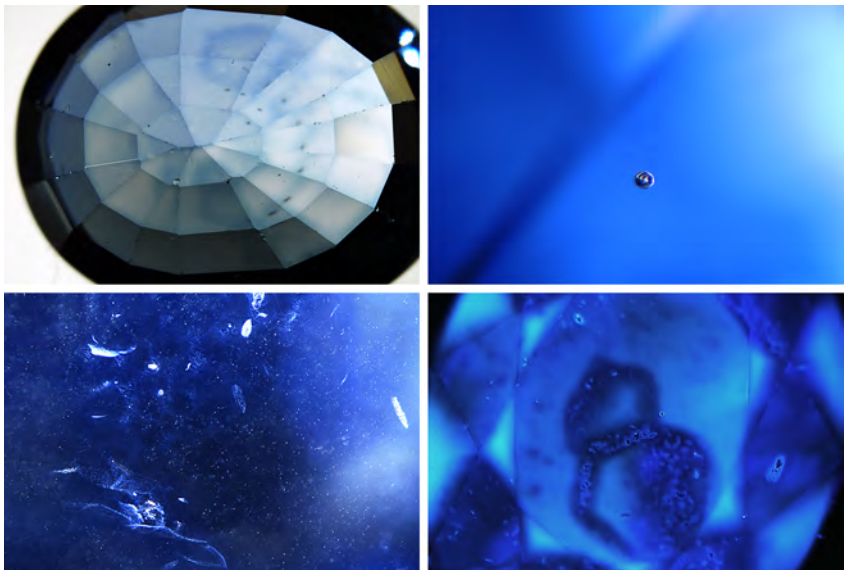

Figure 23. Top left: Color concentration was seen along the pavilion facet junctions of the synthetic sapphire, and blue halos were shown on the table facet. Top right: A spherical gas bubble was observed. Bottom left: Numerous clouds were visible throughout the stone. Some formed fingerprint-like patterns. Bottom right: Under the DiamondView's short-wave UV radiation, blue fluorescence was absent where there were concentrations of the diffusion color in the stone. Fields of view: 9.61 mm (top left), 1.25 mm (top right), 2.9 mm (bottom left), and 8.58 mm (bottom right).

properties were consistent with heated sapphire, either natural or synthetic. Under magnification and diffused transmitted lighting, a blue color concentration was observed along the facet junctions on both the pavilion and crown facets, along with a few large blue halos on the table facet (figure 23, top left), which indicated that the stone had been titanium diffused (R.E. Kane et al., "The identification of blue diffusion-treated sapphire," Summer 1990 *G&G*, pp. 115–133; Summer 2015 GNI, pp. 203–205). Under darkfield lighting, individual large spherical gas bubbles were present (figure 23, top right). Numerous clouds observed throughout much of the stone could have easily been mistaken for natural clouds. Some of them grouped to form natural-looking fingerprint-like inclusions (figure 23, bottom left). The stone's internal characteristics indicated a melt-grown synthetic origin. However, when immersing in methylene iodide under crossed polarizers and viewing down the optic axis, no Plato lines were observed (see W. Plato, "Oriented lines in synthetic corundum," Fall 1952 *G&G*, pp. 223–224). The absence of Plato lines does not rule out flame-fusion growth. The heat from diffusion treatment can reduce the visibility of Plato lines (S. Elen and E. Fritsch, "The separation of natural from synthetic colorless sapphire," Spring 1999 *G&G*, pp. 30–41). More advanced testing is needed to reveal all the physical and chemical properties of this unique stone.

Under the short-wave radiation (a 20-nm-wide band centered at 225 nm) in a DiamondView device, the stone displayed a strong chalky blue fluorescence. Hughes and Emmett (2005) concluded that the chalky blue fluorescence was due to isolated Ti^{4+} ions, or Ti-Al vacancy pairs. The strength of the chalky fluorescence depends on the growth temperature and Ti^{4+} concentration relative to other impurities. In melt-grown corundum, the high growth temperature allows Ti^{4+} to pair with Al vacancies more easily than other charge compensating ions; this creates the chalky fluorescence. In contrast, Pairing of Ti^{4+} with other ions (usually Fe^{2+} or Mg^{2+}) and the presence of Fe^{3+} ions prevent fluorescence. That could explain why the chalky fluorescence was not present where the blue diffusion color was concentrated (R. Hughes and J. Emmett, "Heat seeker: UV fluorescence as a gemological tool," 2005, www.ruby-sapphire.com/heat_seeker_uv_fluorescence.htm).

LA-ICP-MS analysis was performed on the girdle of the stone. Three laser ablation spots were drilled six times down into the stone. The concentration vs. depth profile is shown in figure 24. From the surface of the stone to around 180 µm depth, the Be concentration decreased from 76.8 to 13.9 ppma, Mg from 7.8 to 0.8 ppma, Ti from 580 to 391 ppma, Fe from 390 to 83.4 ppma, and Ga from 6.12 to 1.36 ppma. The results confirmed diffusion treatment, not only by Ti and Fe but also by Be, Mg, and Ga. The presence of Mo provided some indication of synthetic origin. In a GIA identification report, the stone was described as titanium and beryllium diffused. It is the first time GIA has examined a multi-elemental diffused and melt-grown synthetic sapphire.

Ziyin Sun, Jonathan Muyal, and Nicole Ahline

TOURMALINE

Paraíba Tourmaline with Unusual Coating

Paraíba tourmaline, named after the Brazilian state where it was discovered in the late 1980s, is a precious copper-bearing tourmaline variety (e.g., J.E. Shigley et al., "An update on 'Paraíba' tourmaline from Brazil," Winter 2001 *G&G*, pp. 260–276). Treatments such as heating and clarity enhancement have been described (e.g., S.F. McClure et al., "Gemstone enhancement and its detection in the

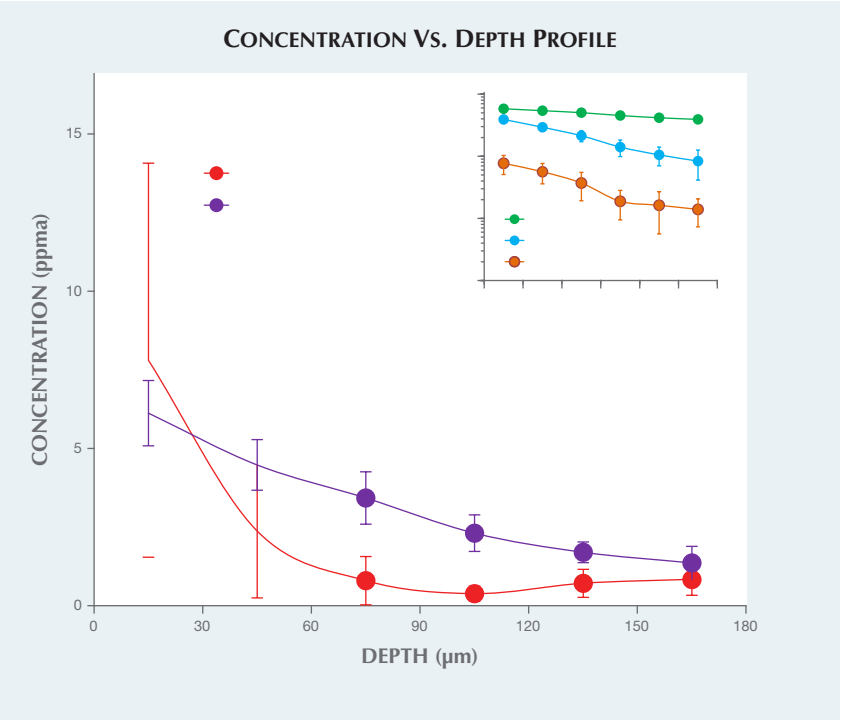

Figure 24. The synthetic sapphire's concentration vs. depth profile revealed that concentrations of Be, Mg, Ti, Fe, and Ga decreased significantly when the laser ablation spots went deeper into the stone.

2000s," Fall 2010 *G&G*, pp. 218–240), but coating has never been reported.

A Paraíba tourmaline ring with an unusual coating was recently submitted to GIA's Tokyo laboratory for identification and origin service (figure 25). Standard gemological properties revealed an RI of 1.640–1.620, consistent with tourmaline. The stone showed medium to strong dichroism displaying greenish blue and light blue colors. Natural inclusions such as trichites and fingerprints were observed. We identified the stone as tourmaline using Raman spectroscopy. EDXRF and UV-Vis spectroscopy were performed to confirm the presence of copper within the material, as well as the material's cause of color.

Viewed face-up with the unaided eye, the stone appeared normal. However, the coated surface looked different under reflected lighting and darkfield illumination (figure 26, left). A brassy, uneven submetallic luster was observed under reflected light, while whitish features in the submetallic luster area (figure 26, right) appeared under darkfield illumination. Coatings typically show signs of wear due to their low durability. This is often seen at the facet junctions. This coating did not show signs of wear and could not be removed using a standard ink pen eraser.

LA-ICP-MS chemical analyses detected elements such as B, Li, and Na, indicating elbaite tourmaline. However, strong early (near-surface) peaks of elements Pt, W, and Mo, which are not normally contained in natural tourmaline, were detected. We determined that this chemistry difference probably resulted from the submetallic surface coating. As with Pt- and Pt-related coatings, it is possible that the coating was used to improve abrasion resistance (e.g., K. Schmetzer, "Surface treatment of gemstones, especially topaz – an update of recent patent literature," *Journal of Gemmology*, Vol. 31, No. 1, 2008, pp. 7–13)

Figure 25. The Paraíba tourmaline in this ring had an unusual submetallic surface coating.

Figure 26. Left: An uneven submetallic coating with an irregular pattern is revealed with reflected light. The white dashed box represents the area shown in the right photo. Field of view 3.33 mm. Right: Under brightfield illumination, a part of the left table facet shows whitish surface structures surrounding the metallic luster domains. Field of view 1.31 mm.

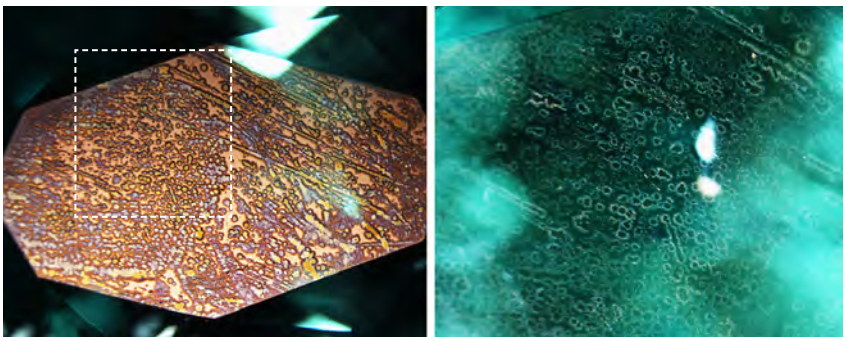

or to assist with scanning electron microscopy (SEM) observation (e.g., I. Stokroos et al., "A comparative study of thin coatings of Au/Pd, Pt and Cr produced by magnetron supporting for FE-SEM," *Journal of Microscopy*, Vol. 189, No. 1, 1998, pp. 79–89).

The reason for applying this coating is unknown. This is the first time GIA's laboratory has observed coated Paraíba tourmaline.

Kazuko Saruwatari and Philip G. York

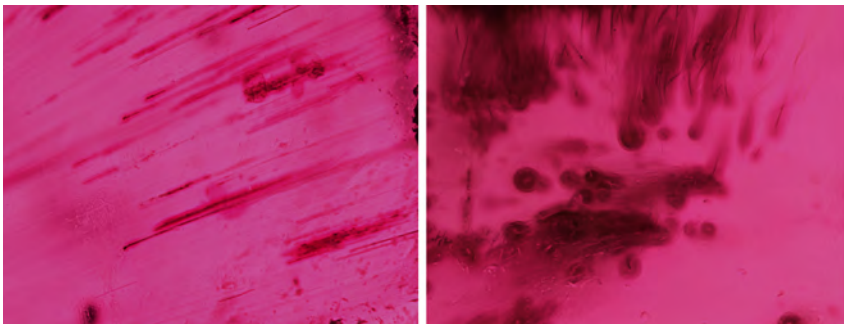

Figure 27. Left: Surface-reaching growth tubes and fractures associated with strong pink sleeves, whose color became weaker as they penetrated the stone's interior; field of view 2.83 mm. Right: Looking down the length of the growth tubes, bleeding of pink color was observed; field of view 1.13 mm.

RUBELLITE with Incredibly Strong "Pink Sleeves"

GIA's Hong Kong laboratory recently examined a purplish red cabochon-cut rubellite tourmaline. Standard gemological tests yielded a spot RI of 1.64 and SG of 3.06, which are consistent with tourmaline. Magnification revealed strong doubling, fluid inclusions, and parallel growth tubes, all typical of tourmaline. What made this specimen unusual were its localized zones of strong pink coloration surrounding surface-reaching growth tubes and fractures (figure 27, left). Bleeding of pink color from the growth tubes into the body of the stone was best observed looking down the length of the growth tubes (figure 27, right); the pink color gradually faded away into the surrounding tourmaline host. This type of zoning has come to be known as "pink sleeves." It is different from dye concentrations, which would only be located inside the surface-reaching growth tubes and fractures.

Radiation-induced pink sleeves surrounding surface-reaching growth tubes and fractures have been reported in Paraíba tourmalines from Mozambique. The formation is believed to be due to a radioactive solution entering the growth tubes and fractures by capillary action, and the presence of pink sleeves proves that the stone has not undergone heat treatment. (J.I. Koivula et al., "Solution-generated pink color surrounding growth tubes and cracks in blue to blue-green copper-bearing tourmalines from Mozambique," Spring 2009 *G&G*, pp. 44–47). To the best of our knowledge, the incredibly strong pink sleeves seen in this rubellite have not been previously reported in either Paraíba or rubellite tourmaline.

Xiaodan Jia and Mei Mei Sit

PHOTO CREDITS:
Robison McMurtry—1, 12; Jian Xin (Jae) Liao—2, 18; Augusto Castillo—4; Sood Oil (Judy) Chia—6; Kyaw Soe Moe—7 (right); Nuttapol Kitdee—9, 14; Charuwan Khowpong—10, 11, 16, 17; Ungkhana Atikarnsakul—17; Paul Johnson—19, 21; Jonathan Muyal—23; Nicole Ahline—23; Masumi Saito—25; Kazuko Saruwatari—26; Xiaodan Jia—27.